ELSEVIER

Journal of Alloys and Compounds 234 (1996) 218–224

Journal of ALLOYS AND COMPOUNDS

Mechanical damping effects by flux lines in $YBa_2Cu_3O_{7-x}$ and $Bi_2Sr_2CaCu_2O_{8+\delta}$ thin films

C. Hünnekes, H.G. Bohn

Institut für Festkörperforschung, Forschungszentrum Jülich GmbH, D-52425 Jülich, Germany

Received 23 June 1995

Abstract

Internal friction (IF) measurements of epitaxial $YBa_2Cu_3O_{7-x}$ and $Bi_2Sr_2CaCu_2O_{8+\delta}$ thin films were carried out in magnetic fields up to 2.8 T. By measuring at constant temperature and magnetic fields applied perpendicular to the crystallographic c axis the lower critical field $H_{c_1}^{\perp}$ for the $YBa_2Cu_3O_{7-x}$ films was determined. For all film thicknesses between 43 nm and 600 nm values of 25 ± 3 mT at 20 K and 14 ± 3 mT at 50 K were found.

For the $Bi_2Sr_2CaCu_2O_{8+\delta}$ films the IF was measured as a function of temperature for constant magnetic field H. For both $\boldsymbol{H} \perp \boldsymbol{c}$ and $\boldsymbol{H} \| \boldsymbol{c}$ a maximum in the IF was found which can be quantitatively explained within the model of thermally activated flux diffusion. The activation energy for the diffusion varies as $H^{-0.3}$ for $\boldsymbol{H} \perp \boldsymbol{c}$ and $H^{-0.9}$ for $\boldsymbol{H} \| \boldsymbol{c}$.

Keywords: High temperature superconductivity; Lower critical field; YBCO; Bi2212; Internal friction

1. Introduction

In many of the applications of the high temperature superconductors the pinning of flux lines (FLs) plays an important role. Since on the one hand FLs interact with the applied field while on the other hand they are pinned to the crystal lattice, internal friction (IF) measurements provide an excellent tool for studying energy dissipation due to FL movement. Because the type of the FLs in the high temperature superconductors is strongly influenced by the highly anisotropic structure of the crystalline lattice (i.e. layered structures with different arrangements of the layers) it is very interesting to compare different materials. Here we will present IF measurements on $YBa_2Cu_3O_{7-x}$ (YBCO) and $Bi_2Sr_2CaCu_2O_{8+d}$ (Bi2212) thin films. In order to quantify the anisotropy the ratio of the coherence lengths within the planes and perpendicular to them may be taken. While this is relatively low for YBCO the Bi2212 superconductor has a anisotropy which is higher by more than a factor of 10 [1]. While the structure of the FLs in YBCO is comparable with that of conventional superconductors for the case of Bi2212 they consist of "flux disks" which are located in the superconducting a–b planes. Their arrangement is complex and results in an interesting new magnetic phase diagram [2].

While IF measurements have been carried out extensively on sintered ceramics and single crystals (for a review see Ref. [3]) only a few studies on thin films are known [4–11]. In this paper we present a determination of the lower critical field field $H_{c_1}^{\perp}$ of thin YBCO films by means of IF measurements. This method has previously been applied to other superconducting materials [12,13]. Moreover, new investigations on thin Bi2212 films will be reported and compared with published results from YBCO films [11].

2. Experimental details

Both the YBCO and Bi2212 films were deposited by a d.c. sputtering technique [14,15] onto single-crystal $LaAlO_3$ or $NdGaO_3$ (YBCO) and $SrTiO_3$ (Bi2212) substrates. The films grew epitaxially on these substrates with the crystallographic c axis perpendicular to the substrate surface. From channeling measurements minimum yields of typically 3% (YBCO) and

SSDI 0925-8388(95)02036-5

Table 1
Summary of the sample data

	YBCO	Bi2212	
		Sample A	Sample B
Film thickness (nm)	43, 50, 100, 275, 300, 600	330	330
Substrate	$LaAlO_3$ or $NdGaO_3$	$SrTiO_3$	$SrTiO_3$
T_c^{mid} (K)	90.6–92.8	95	93
Transition width (K)	Typically 0.7	≈10	≈10

9% (Bi2212) respectively were obtained indicating the high degree of epitaxy. The films covered an area of about 1 cm^2.

YBCO films with thicknesses t_s of 43 nm, 50 nm, 100 nm, 275 nm, 300 nm and 600 nm were produced. The midpoint of the resistive transition was between 90.6 K and 92.8 K indicating $x < 0.1$ [16] and the width of the transition was typically 0.7 K. No influence of the different substrates used was observed.

Two Bi2212 films with a thickness of 330 nm were deposited onto $SrTiO_3$ substrates. From the resistive transition $T_c^{mid} \approx 95$ K (sample A) and $T_c^{mid} \approx 93$ K (sample B) and a transition width of approximately 10 K were obtained. The difference in the critical temperature is due to the different oxygen content of the samples [15]. The sample data are summarized in Table 1.

The samples were glued to the end of a low damping Si cantilever oscillator (Fig. 1). This mechanical oscillator was driven into resonant vibrations by an electrostatic drive system. The frequency of the sample vibration was near 250 Hz, and the amplitude was 400 nm. The IF was determined from the free decay of the oscillation after switching off the excitation.

Magnetic fields H up to 2.8 T were applied parallel to the cantilever. The YBCO samples were glued onto the cantilever with their main plane parallel to $\boldsymbol{H}$ (see Fig. 1(a)), denoted in the following as $\theta = 0°$, *i.e.* $\boldsymbol{H} \perp \boldsymbol{c}$.

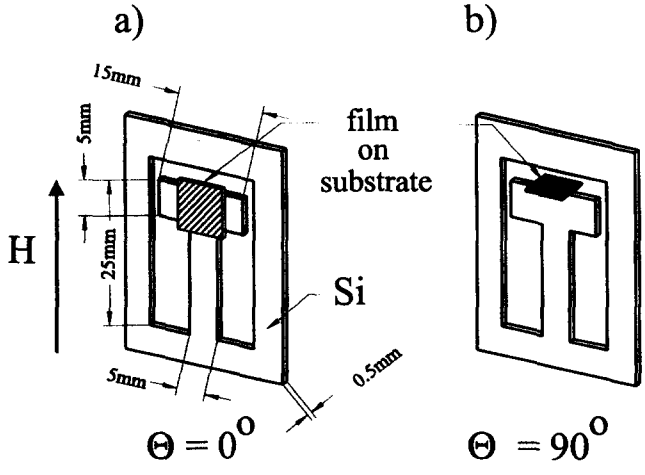

Fig. 1. Schematic drawing of the two possible measuring geometries. $\theta = 0°$ belongs to $\boldsymbol{H} \perp \boldsymbol{c}$ while $\theta = 90°$ yields $\boldsymbol{H} \| \boldsymbol{c}$.

The Bi2212 samples were measured in this geometry and were additionally mounted in a perpendicular arrangement (i.e. $\theta = 90°$, see Fig. 1(b)). In this geometry $\boldsymbol{H}$ is parallel to the c axis. In both positions the sample can be tilted with respect to the magnetic field by ±10°. All angles θ were measured by means of a Hall detector and could be determined with an accuracy $\Delta\theta = \pm 0.5°$ and $\Delta\theta = \pm 0.7°$ for $\theta \approx 0°$ and $\theta \approx 90°$ respectively. The errors are due to possible misalignments between sample and Hall detector.

3. Theoretical background

If a superconductor oscillates in an applied magnetic field both the resonance frequency and the damping of the vibration are affected. In the Meissner state the resonance frequency f will increase from its zero field value $f_0 = f(H = 0)$ owing to an extra restoring force which tries to align the superconductor along the applied magnetic field. For a thin superconducting film oscillating in a field applied in the plane of the film the increased frequency f_i is given by [7]

$$f_i = f_0\left[1 + \frac{Pl}{(2\pi f_0)^2 I}\right]^{1/2} \quad (1)$$

where P is a line tension due to surface screening currents, l is the length of the oscillator and I is the effective moment of inertia of the Si oscillator/sample assembly. P is a function of the applied field [7]:

$$P = \pi\left(\frac{w_s}{2}\right)^2 \frac{l_s}{l} \mu_0 H^2 \text{ (for } \theta = 0°) \quad (2)$$

where l_s and w_s are length and width respectively of the superconducting sample. The effective moment of inertia I can be calculated either from the geometry of the oscillator or from the frequency at fields below H_{c_1} using Eqs. (1) and (2). Both methods consistently provide $I \approx 140$ g mm^2 for the samples used here. If FLs enter the sample and move relative to it, $f(H)$ will be reduced relative to f_i owing to a reduction in the line tension P [17]. In addition, damping occurs when FLs move relative to the lattice [17]. In the experiments presented here this movement is caused by an interaction between surface screening currents and the

FLs. FL pinning in high temperature superconductors is very weak even at low temperatures. Thus the point where the damping starts to increase with the applied field indicates the onset of penetration of flux into the sample. This experimental technique provides a means to determine the lower critical field $H_{c_1}^{\perp}$: $H_{c_1}^{\perp}$ is the field where both the resonance frequency $f(H)$ starts to deviate from f_i (Eq. (1)) and the damping starts to rise.

In general the damping Q^{-1} is defined as

$$Q^{-1} = \frac{\Delta W_{sl}}{2\pi W_m} \tag{3}$$

where ΔW_{sl} is the energy dissipated per cycle and W_m the maximum elastic energy stored in the oscillator. W_m can be calculated for the oscillator sketched in Fig. 1 using the appropriate elastic constants as $W_m \approx a_0^2 \times 3.4 \times 10^2\ \mathrm{J\,m^{-2}}$ (a_0, amplitude of oscillation). For the case discussed here ΔW_{sl} is the energy dissipated by the diffusional movement of FLs relative to the sample which can be calculated after Refs. [18,19] as

$$\Delta W_{sl} = \pi V_s \chi'' \mu_0 \langle H_{ac}^2 \rangle \tag{4}$$

where $V_s = w_s l_s t_s$ is the volume of the superconducting film, χ'' is the imaginary part of the a.c. susceptibility and

$$\langle H_{ac}^2 \rangle = 6.16 \times 10^4 \left(\frac{\pi w_s}{4 t_s} \cos^2\theta + \sin^2\theta \right) a_0^2 H^2 \tag{5}$$

is the time- and space-averaged a.c. field [18] calculated for the measuring geometry used here. This a.c. field arises from the oscillation of the superconductor in the uniform magnetic field. The factor $\pi w_s / 4 t_s$ accounts for stray fields caused by surface screening currents if H is applied parallel to the surface of the film (i.e. $\theta = 0°$) [18]. χ'' can be calculated after Kes et al. [20] using relaxation times [18]

$$\tau = \left(\frac{l_s}{\pi} \right)^2 \frac{4 t_s}{\pi w_s} \frac{\mu_0}{\rho} \qquad (\theta = 0°) \tag{6}$$

$$\tau = \left(\frac{t_s}{\pi} \right)^2 \frac{\mu_0}{\rho} \qquad (\theta = 90°) \tag{7}$$

where ρ is the resistivity. τ depends on the orientation of the sample with respect to the magnetic field (see Fig. 1). For $\theta = 0°$ the FLs move along the length of the superconductor and again the stray field factor $\pi w_s / 4 t_s$ shows up. When H is applied parallel to the main area of the superconducting film ($\theta = 90°$) no stray fields are generated and the flux moves along the thickness of the superconductor.

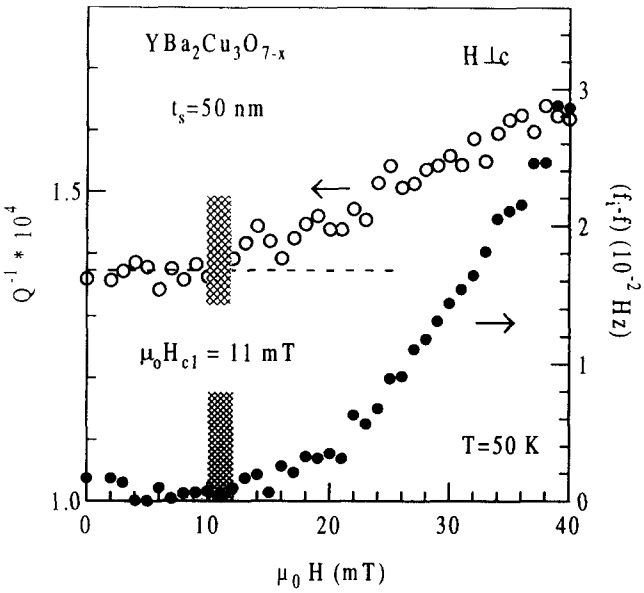

Fig. 2. IF and difference $f_i - f$ between calculated (f_i, Eq. (1)) and measured resonance frequency f as a function of the applied field for a 50 nm thick $YBa_2Cu_3O_{7-x}$ film at 50 K. The field where the IF starts to rise with H and where f deviates from f_i is identified as $H_{c_1}^{\perp}$ yielding $\mu_0 H_{c_1}^{\perp} \approx 11$ mT.

4. Results and discussion

4.1. Determination of $H_{c_1}^{\perp}$ of $YBa_2Cu_3O_{7-x}$ films

Fig. 2 shows both Q^{-1} (open circles, left-hand scale) and the difference between f_i calculated from Eqs. (1), (2) and the measured frequency f (full circles, right-hand scale) as a function of the applied field at $T = 50$ K for the 50 nm thick YBCO film. For fields lower than about 11 mT Q^{-1} is independent of the applied field while above the damping increases. f_i equals f for H smaller than 11 mT indicating that the sample is in the Meissner state. For higher fields f deviates from f_i. From both the IF and the frequency measurement one concludes that above 11 mT FLs have penetrated into and move within the sample. Thus the lower critical field $H_{c_1}^{\perp}$ is determined as 11 mT for this sample. Similar results were obtained for the other samples. For all film thicknesses between 43 nm and 600 nm (see Table 1) we obtained $H_{c_1}^{\perp}(50\,\mathrm{K}) = 14 \pm 3$ mT and $H_{c_1}^{\perp}(20\,\mathrm{K}) = 25 \pm 3$ mT independent of the film thickness. These results are in very good agreement with data from single crystals where $H_{c_1}^{\perp}(0, \mathrm{K}) \approx 25$ mT has been extrapolated from measurements between T_c and 4.2 K [21,22].

4.2. $Bi_2Sr_2CaCu_2O_{8+\delta}$

4.2.1. $H_{c_1}^{\perp}$

The temperature dependence of the IF of thin YBCO films at constant magnetic fields has been discussed before within the model of thermally as-

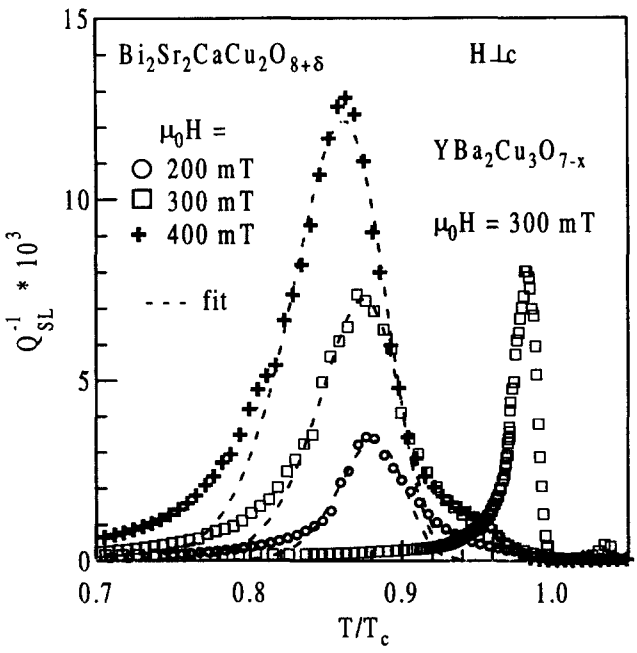

Fig. 3. Q_{SL}^{-1} as a function of temperature T at fixed magnetic fields of 200 mT, 300 mT and 400 mT for a 330 nm thick $Bi_2Sr_2CaCu_2O_{8+\delta}$ film (sample A) at $H \perp c$. ---, fits according to Eqs. (3)–(6), (8), (9).

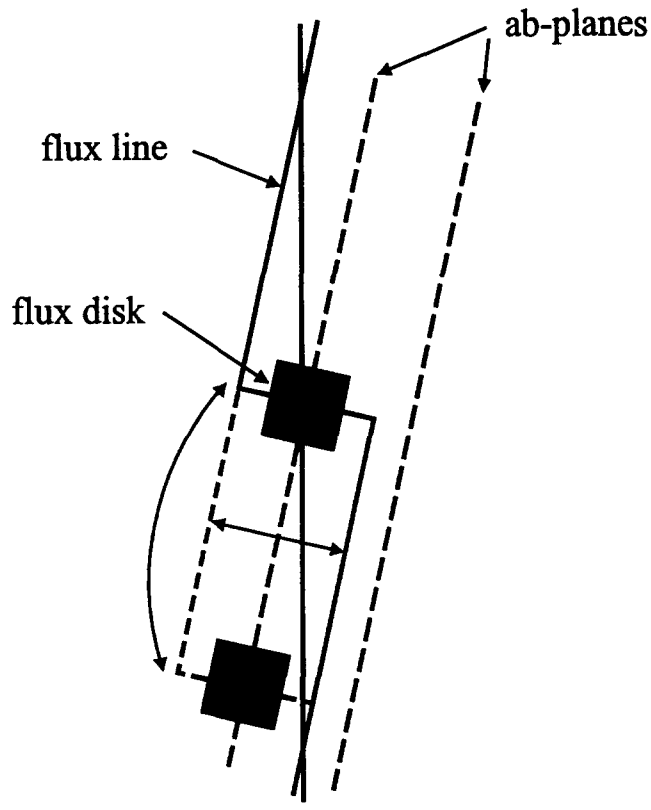

Fig. 4. Schematic drawing of the flux movement for $\theta \approx 0°$C: The flux line is moved from the left to the right and back again by a displacement of a flux disk in the a–b planes.

sisted flux flow (TAFF) [11]. In this contribution we present data for Bi2212 films. Fig. 3 shows the damping Q_{sl}^{-1} (defined as the difference between the damping at constant H and the zero field damping, i.e. only the damping due to FL movement) as a function of the reduced temperature T/T_c for $\theta = 0°$ and three different values of the applied field. Data are from sample A. A broad maximum is observed near $T/T_c \approx 0.86$. The position shifts slightly to lower temperatures with increasing field and height and width of the maximum rise. For comparison the data for a 300 nm thick YBCO film at 300 mT are also shown. Obviously the corresponding maximum for the Bi2212 film has a similar height, but is much broader and located at lower reduced temperature.

In Bi2212 the FLs form flux disks which are located in the superconducting layers. The coupling of these flux disks along the c direction is still under discussion. Even for the geometry discussed here ($\theta = 0°$, i.e. field applied along the superconducting planes) a slight misorientation of the sample with respect to the magnetic field would cause flux disks. The movement of flux along the c direction is then brought about by a displacement of a single flux disk (Fig. 4). Thus the maximum in Q^{-1} is caused by the movement of flux disks in the superconducting layers. In analogy to our analysis of the YBCO data we will show that this movement can be described by the TAFF model too.

The IF was calculated from Eqs. (3)–(6). The resistivity ρ which enters into Eq. (6) was taken as

$$\rho_{TAFF} = \rho_0 \exp(-U/kT) \tag{8}$$

with a temperature- and field-dependent activation energy $U = U(H, T)$ given by [23]

$$U = U_0(H)(1 - T/T_c)^{3/2} \tag{9}$$

A log-normal distribution [24] for $U_0(H)$ accounts for different types of pinning sites and influences the width of the damping peak. From a fit of this theory to the experimental data the mean value $U_{0m}(H)$ of the energy distribution is obtained. The width of the distribution turned out to be constant with a value of $U_{FWHM}/U_{0m} = 0.77$. The broken lines in Fig. 3 represent fits to the data. The agreement between measurement and calculation is fairly good.

Fig. 5 shows U_{0m} as a function of the applied field H for both measured samples. The field range accessible in these experiments is limited to 100 mT–450 mT by the damping measurement: the applied field must be sufficiently high in order to distinguish Q_{sl}^{-1} from the background damping of typically 10^{-4}, and the high field limit is given by the maximum damping of approximately 2×10^{-2} which can be measured by the apparatus. In this range a field dependence of $U_{0m} \propto H^{-0.3}$ is found for both samples while the absolute value of U_{0m} differs by a factor of approximately 2.5. The higher activation energies were found

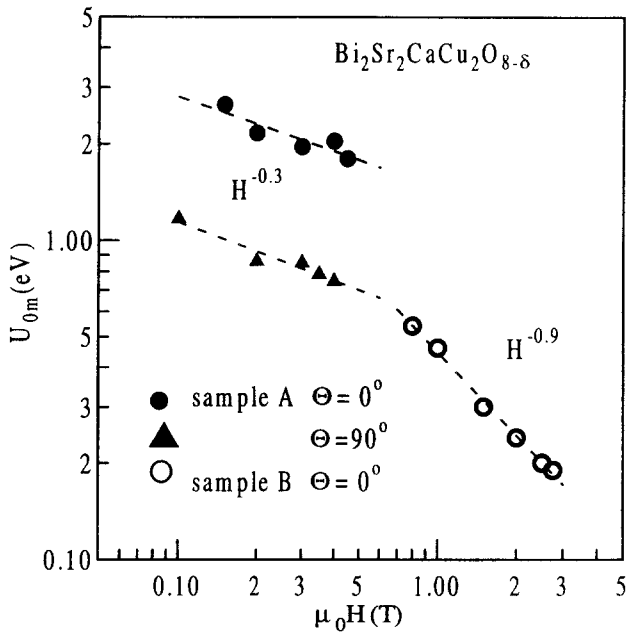

Fig. 5. Mean value of the energy distribution of $U_0(H)$ as a function of H for two $Bi_2Sr_2CaCu_2O_{8+\delta}$ films in the directions $\boldsymbol{H}\perp\boldsymbol{c}$ and $\boldsymbol{H}\|\boldsymbol{c}$. ---, best fits and represent the scaling of $U_{0m}(H)$.

for sample A which also exhibits the higher transition temperature T_c. Since both T_c and U_{0m} are known to be sensitive to the oxygen content of the sample [25,26] sample A seems to be better optimized with respect to T_c.

The same field dependence of the activation energy has been found before for Bi2212 single crystals [27]. Here the absolute value of U_0 is smaller by a factor of 5 than the activation energy of sample B. This seems to be reasonable in view of the fact that single crystals possess a much lower defect density than thin films which would result in a lower pinning energy.

The YBCO thin films, for comparison, obey a dependence of $U_{0m} \propto H^{-1}$. The absolute value at for example 0.4 T is more than a factor of 10 higher than for the Bi2212 film A. This shows that for $\boldsymbol{H}\perp\boldsymbol{c}$ and for the field range investigated here the pinning in YBCO is much stronger than in Bi2212.

4.2.2. $\boldsymbol{H}\|\boldsymbol{c}$

The change in the resonance frequency f with temperature is plotted in Fig. 6(a). At zero field (full line) the decrease in f with increasing temperature is due to the temperature dependence of the elastic modulus of the Si oscillator. When a magnetic field of 1.5 T is applied parallel to the c axis the frequency increases in three steps positioned at 44 K, 67 K and 82 K. The corresponding IF is shown in Fig. 6(b). A clear maximum shows up at 44 K corresponding to the step in the frequency, and also a slight irregularity in the damping is found at 67 K.

One may speculate that the frequency step at 82 K

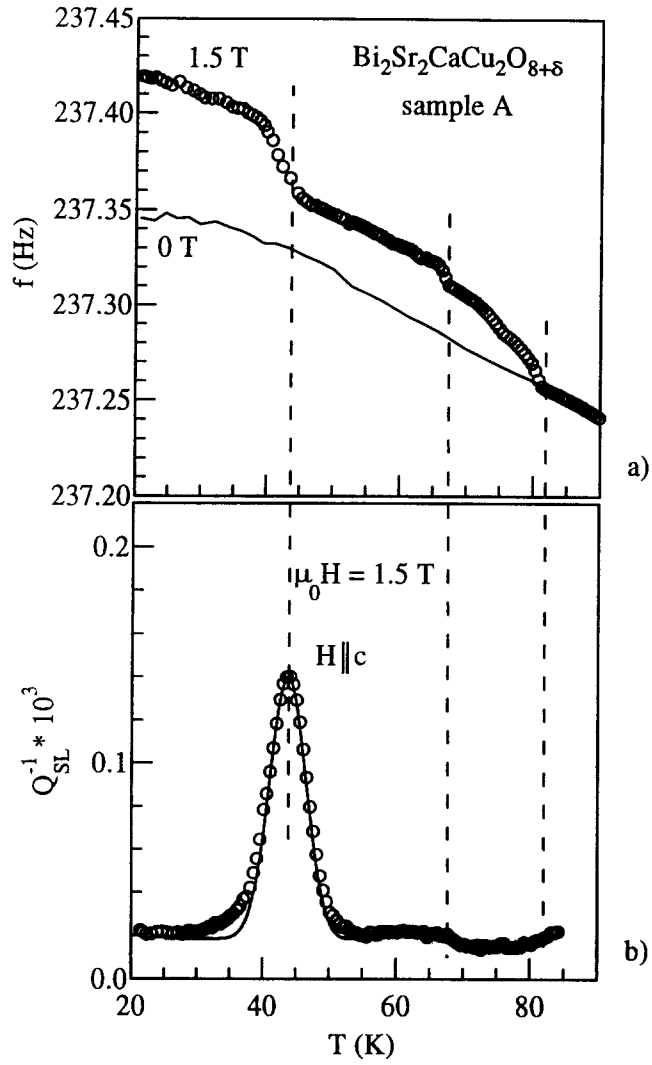

Fig. 6. Change in (a) the measuring frequency f and (b) the damping Q^{-1} as a function of temperature at mixed fields of 0 T (only for f) and 1.5 T parallel to the c axis of a $Bi_2Sr_2CaCu_2O_{8+\delta}$ film (sample A). The solid line in the damping spectrum is a fit according to Eqs. (3)–(5), (7)–(9).

originates from a two-dimensional to three-dimensional cross-over of the FL arrangement which increases the stiffness of the FL lattice. It is possible that above 82 K the correlation between the flux disks of neighbouring superconducting layers is lost. This transition has been discussed in the literature [2]. Around 82 K no effect in Q^{-1} is observed because the dissipated energy of the FL movement is too small to be detected in our experiment.

The frequency step and the maxima in Q^{-1} at 67 K and 44 K have the same origin. At both temperatures thermally activated flux disks influence damping and frequency. Two different maxima show up because different diffusion modes have to be considered.

(1) At 67 K the step in f and the maximum in Q^{-1} are caused by a remaining field component $\boldsymbol{H}\perp\boldsymbol{c}$ due to a small misalignment between sample and applied field. In this case the relaxation time given

by Eq. (6) describes the flux movement. This can be proven when the temperature position of the maximum discussed above for $\boldsymbol{H} \perp \boldsymbol{c}$ is extrapolated to the field applied here: for sample A one finds (see Fig. 5) $U_{0m}(1.5\,\mathrm{T}) \approx 1.3$ eV which results in a depinning temperature of 66 K in excellent agreement with the measured temperature of 67 K.

(2) At 44 K flux diffusion along the thickness of the sample causes the maximum in Q^{-1} as well as the step in f. As explained above no stray fields and a different diffusion length have to be considered (see Eq. (7)). The effects then can be explained within the TAFF model. Taking Eqs. (3)–(5) and (7)–(9) and a log-normal distribution of $U_0(H)$ with $U_{FWHM}/U_{0m} = 0.35$ the maximum in Q^{-1} can be perfectly described by the theory outlined above as shown in Fig. 6(b) where the solid line represents the best fit to the data.

$U_{0m}(H)$ as obtained for $\boldsymbol{H} \| \boldsymbol{c}$ is also included in Fig. 5. U_{0m} varies as $H^{-0.9}$. Unfortunately, in this case the accessible field range has its lower limit at 0.8 T. Thus there are no data of U_{0m} for $\boldsymbol{H} \| \boldsymbol{c}$ and $\boldsymbol{H} \perp \boldsymbol{c}$ in the same field range. Nevertheless it can be seen from Fig. 5 that the pinning of FLs in the geometry $\boldsymbol{H} \| \boldsymbol{c}$ is much weaker than for the perpendicular orientation. A possible explanation could be that the displacements of the "flux disks" which occur in the $\boldsymbol{H} \| \boldsymbol{c}$ orientation are substantially smaller than in the perpendicular orientation. Because of the spatial dependence of U this results in different $U_0(H)$ when spatially averaged over the displacements.

In contrast to our data, for single crystals dependences of $U_0 \propto H^{-0.3}$ [27] and $U_0 \propto H^{-0.6}$ [28] are reported in the literature with absolute values 5 [28] to 10 times [27] smaller than those found in the present experiments. This difference could be ascribed to different oxygen contents and/or different defect densities of the samples which change the pinning energy drastically [25,26].

The low temperature damping peak substantially increases when θ deviates from 90°C while its position changes little. This increase is due to the onset of surface screening currents which are created by a field component parallel to the surface of the film. These surface currents dominate the FL movement in thin films because their force acting on the FLs is by a factor of $\pi w_s / 4 t_s \approx 2 \times 10^4$ enhanced over forces due to the elastic stiffness of the FL lattice [18]. In Fig. 7 the maximum damping $Q^{-1}_{max} = Q^{-1}(T_{max})$ is plotted vs. θ for $\mu_0 H = 2$ T. When changing θ from 90° to 82° Q^{-1}_{max} rises by two orders of magnitude. These data can be compared with the theory of linear flux diffusion. By inserting the angular dependence of the time- and space-averaged a.c. field $\langle H^2_{ac} \rangle$ (Eq. (5)) into Eq. (4) and taking $\chi'' = \chi''_{max} = 0.41723$ [20] the dissipated energy can be calculated. As shown in Fig. 7 the measured data approach the theoretical curve very well. As the background damping in the temperature region cannot be determined uniquely (see Fig. 6) the true Q^{-1}_{max} is smaller than the calculated damping. Nevertheless, thermally activated FL diffusion accounts for the shape of the low temperature dissipation maximum as well as for the dependence of its height on the tilt angle θ.

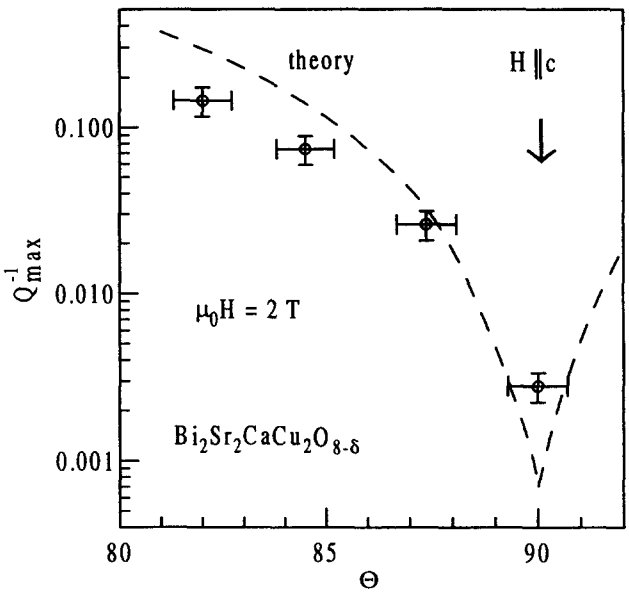

Fig. 7. Maximum damping Q^{-1}_{max} as a function of the tilt angle θ of the samples. At $\theta = 90°$ H is parallel to the c axis.

Similar measurements on single crystals have been published before by Duran et al. [29]. They explain the maximum at lower temperatures by a softening of the interaction between the FL disks in the a–b plane while the maximum at higher temperatures is attributed to a complete depinning of the FL disks. For thin films our experiments have shown that both maxima can be quantitatively explained by thermal diffusion of FLs.

5. Summary and conclusions

From both the magnetic field dependence of the resonance frequency f and the damping Q^{-1} the lower critical field $H^{\perp}_{c_1}$ for $YBa_2Cu_3O_{7-x}$ thin films was determined. For films with thickness between 43 nm and 600 nm a value of $H_{c_1} = 14 \pm 3$ mT for $T = 50$ K and 25 ± 3 mT for 20 K was obtained in good agreement with data obtained for single crystals.

The IF of $Bi_2Sr_2CaCu_2O_{8+\delta}$ thin films exhibits a low temperature maximum for $\boldsymbol{H} \| \boldsymbol{c}$ and a maximum located at higher temperatures for $\boldsymbol{H} \perp \boldsymbol{c}$. Both maxima can be quantitatively explained within the model of

thermally activated depinning of flux disks which are located in the superconducting layers.

Acknowledgement

Dr. C. Osthöver is gratefully acknowledged for supplying the Bi2212 samples used in this work.

References

[1] G. Burns, *High Temperature Superconductivity*, Academic Press, New York, 1992, p. 156 ff.
J.C. Martinez, S.H. Brongersma, A. Koshelev, B. Ivlev, P.H. Kes, R.P. Griessen, D.G. de Groot and Z. Tarnavski, *Phys. Rev. Lett., 69* (1992) 2276.
[2] Y.M. Wan, S.E. Hebboul and J.C. Garland, *Phys. Rev. Lett., 72* (1994) 3867.
F. de la Cruz, E. Rodriguez, H. Pastoriza, A. Arribére and M.F. Goffmann, *Physica B, 197* (1994) 596.
[3] P. Esquinazi, *J. Low Temp. Phys., 85* (1991) 139.
[4] S. Gregory, C.T. Rogers, T. Venkatesan, X.D. Wu, A. Inam and B. Dutta, *Phys. Rev. Lett. 62* (1989) 1548.
[5] Y.T. Wen, T.S. Kê, H.G. Bohn, H. Soltner and W. Schilling, *Physica C, 193* (1992) 99.
[6] Y.T. Wen, T.S. Kê, H.G. Bohn, H. Soltner and W. Schilling, *J. Phys.: Condens. Matter, 4* (1992) 4519.
[7] M. Ziese, P. Esquinazi, Y. Kopelevich and A.B. Sherman, *Z. Phys. B, 94* (1994) 265.
[8] M. Ziese and P. Esquinazi, *Physica C, 224* (1994) 79.
[9] M. Ziese, P. Esquinazi and H.F. Braun, *Supercond. Sci. Technol., 7* (1994) 869.
[10] C. Hünnekes, H.G. Bohn, W. Schilling and H. Schulz, *Phys. Rev. Lett., 72* (1994) 2271.
[11] C. Hünnekes, H.G. Bohn, W. Schilling and H. Schulz, *J. Alloys Compd.*, 211–212 (1994) 305.
[12] C. Duran, P. Esquinazi, J. Luzuriaga and E.H. Brandt, *Phys. Lett. A, 123* (1987) 485.
[13] A. Gupta, P. Esquinazi and H.F. Braun, *Physica B, 165–166* (1990) 1443.
[14] U. Poppe, N. Klein, U. Dähne, H. Soltner, C.L. Jia, B. Kabius, K. Urban, A. Lubig, K. Schmidy, S. Hensen, S. Orbach, G. Müller and H. Piel, *J. Appl. Phys.*, 71 (1992) 5572.
[15] C. Osthöver and R.R. Arons, to be published.
[16] H. Theuss and H. Kronmüller, *Physica C, 177* (1991) 253.
[17] E.H. Brandt, P. Esquinazi and H. Neckel, *J. Low Temp. Phys., 63* (1986) 187.
[18] E.H. Brandt, *Phys. Rev. Lett., 68* (1992) 3769.
[19] K.H. Fischer and T. Nattermann, *Phys. Rev. B, 43* (1991) 10372.
[20] P.H. Kes, J. Aarts, J. van der Beek and J.A. Mydosh, *Supercond. Sci. Technol., 1* (1989) 242.
[21] Y. Yeshurun, A.P. Malozemoff, F. Holtzberg and T.R. Dinger, *Phys. Rev. B, 38* (1988) 11828.
[22] S. Sridhar, D.-H. Wu and W. Kennedy, *Phys. Rev. Lett., 63* (1989) 1873.
[23] A.P. Malozemoff, T.K. Worthington, Y. Yeshurun and F. Holtzberg, *Phys. Rev. B, 38* (1988) 7203.
[24] C.W. Hagen and R. Griessen, in A.V. Narlikar (ed.), *Studies of High Temperature Superconductors*, Vol. 3, Nova, New York, 1989, p. 159.
[25] L. Dimesso, R. Masini, M.L. Cavinato, D. Fiorani, A.M. Testa and C. Aurisicchio, *Physica C, 203* (1992) 403.
[26] B. Beschoten, U. Rüdiger, J. Auge, C. Quitmann, H. Frank, H. Kurz and G. Güntherodt, *Physica C, 235–240* (1994) 1373.
[27] T.T.M. Palstra, B. Batlogg, R.B. van Dover, L.F. Schneemeyer and J.V. Waszczak, *Phys. Rev. B, 41* (1990) 6621.
[28] Ph. Seng, R. Gross, U. Baier, M. Rupp, D. Koelle, R.P. Huebener, P. Schmitt, G. Saemann-Ischenko and L. Schultz, *Physica C, 192* (1992) 403.
[29] C. Duran, J. Yazyi, F. de la Cruz, D.J. Bishop, D.B. Mitzi and A. Kapitulnik, *Phys. Rev. B, 44* (1991) 7737.